Inorganic Chemistry

Communication

pubs.acs.org/IC

Tetranuclear Ruthenium(II) Complex with a Dinucleating Ligand Forming Multi-Mixed-Valence States

Shingo Ohzu,[†] Tomoya Ishizuka,[†] Hiroaki Kotani,[†] Yoshihito Shiota,[‡] Kazunari Yoshizawa,[‡,§] and Takahiko Kojima*[,†]

[†]Department of Chemistry, Faculty of Pure and Applied Sciences, University of Tsukuba, Tsukuba, Ibaraki 305-8571, Japan

[‡]Institute for Materials Chemistry and Engineering, Kyushu University, Motooka, Nishi-Ku, Fukuoka 819-0395, Japan

[§]Elements Strategy Initiative for Catalysts & Batteries, Kyoto University, Nishikyo-ku, Kyoto 615-8520, Japan

Supporting Information

ABSTRACT: A square-shaped tetranuclear ruthenium(II) complex, $[Ru^{II}_4Cl_5(bpmpm)_2]^{3+}$ [**1**; bpmpm = 4,6-bis-[[*N*,*N*-bis(2′-pyridylmethyl)amino]methyl]pyrimidine], exhibited four reversible and stepwise one-electron-oxidation processes: chemical oxidation of **1** formed three different mixed-valence states, in one of which the charge is partially delocalized on the two Ru centers, to be evidenced by observation of an intervalence charge-transfer absorption band, categorized into the Robin–Day class II.

Mixed-valence (MV) transition-metal complexes including metal centers in different oxidation states have been investigated to elucidate electronic interactions between the metal centers in light of intermetallic electron transfer.[1−3] The MV species involving weakly coupled (class II) and strongly coupled (class III) metal centers exhibit intervalence charge-transfer (IVCT) bands, which reveal the degree of electronic coupling.[3,4] Recently, MV complexes have been recognized as promising candidates of molecular devices to develop single-molecule magnets,[5] quantum cellular automata,[6] and so on. Along this line, trinuclear and tetranuclear MV complexes using various transition metals have been synthesized, and the optical and magnetic properties have been studied in detail.[7] Among these, Long and co-workers have reported the synthesis of a square-shaped tetranuclear MV complex, $[Ru_4(cyclen)_4(\mu\text{-}pz)_4]^{9+}$ (cyclen = 1,4,7,10-tetraazacyclododecane); however, the characteristics of MV states of the tetranuclear complex have yet to be clarified.[8,9] As for most of the polynuclear complexes forming MV states reported to date, the metal centers in a complex are usually in the same coordination environment, and there are few reports for MV complexes involving transition-metal centers in different coordination environments. In order to explore a new category of MV complexes toward the development of molecular electronics, herein, we report the synthesis and characterization of a novel macrocyclic tetranuclear ruthenium(II) complex using a dinucleating ligand. The tetranuclear ruthenium(II) complex having three kinds of different bridging scaffolds can be oxidized to afford various MV species exhibiting different MV characteristics.

A dinucleating poly(pyridylmethyl)amine ligand, 4,6-bis-[[*N*,*N*-bis(2′-pyridylmethyl)amino]methyl]pyrimidine (bpmpm), was synthesized by condensation of *N*,*N*-bis(2-pyridylmethyl)amine[10] with 4,6-bis(bromomethyl)pyrimidine[11] in CH_3CN.[12] The synthesis of a tetranuclear Ru^{II}-bpmpm complex, $[Ru^{II}_4Cl_5(bpmpm)_2](PF_6)_3$ (**1**), was accomplished through the reaction of $[Ru^{II}Cl_2(p\text{-cymene})]_2$ with bpmpm in EtOH at reflux (Scheme 1). Characterization of **1** was performed

Scheme 1. Synthesis of 1

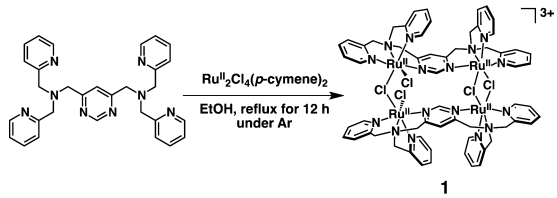

1

using electrospray ionization time-of-flight mass spectrometry (ESI-TOF-MS), ^{1}H NMR spectroscopy, and also X-ray diffraction analysis (see below). The ESI-TOF-MS spectrum of **1** in MeOH exhibited a peak cluster at m/z 866.81 with a peak separation of 0.5, indicating a divalent cation [Figure S1 in the Supporting Information (SI)]. The isotopic pattern of the peak cluster was well matched with the simulated one for the signal of $[\mathbf{1} - 2PF_6]^{2+}$. The ^{1}H NMR spectrum of **1** in CD_3CN at room temperature showed well-resolved aromatic proton signals due to the bpmpm ligand in the range of 7−10 ppm, reflecting the C_2 symmetry of **1** (Figures S2 and S3 in the SI).

A single crystal of **1** suitable for X-ray crystallography was obtained by recrystallization by vapor diffusion of hexane into the acetone solution of **1**. An ORTEP drawing of the cation part of **1** is depicted in Figure 1. As shown in Figure 1, the four Ru^{II} centers are linked through different bridging ligands to form a pseudosquare shape, where Ru1 and Ru2 are bridged by the pyrimidine moiety, Ru1 and Ru1′ are bridged by one μ-chlorido ligand, and Ru2 and Ru2′ are bridged by two μ-chlorido ligands. The asymmetric coordination modes of the Ru1 and Ru2 centers are probably caused by steric repulsion between the two bpmpm ligands in the course of the formation of the bis(μ-chlorido) structure between the Ru1 and Ru1′ centers. The number of counteranions and the bond distances around the Ru centers suggested that the oxidation states of all four Ru centers are 2+.

Received: October 2, 2014
Published: November 20, 2014

   dx.doi.org/10.1021/ic502422u | *Inorg. Chem.* 2014, 53, 12677−12679

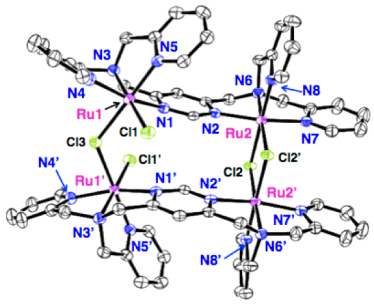

Figure 1. Crystal structure of the cation moiety of **1**. Thermal ellipsoids are shown at the 50% probability level.

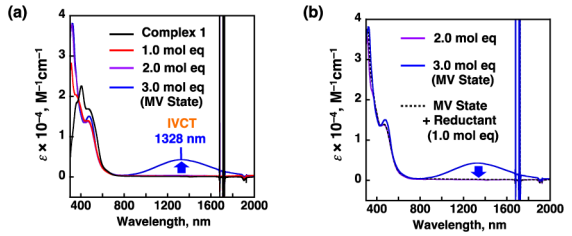

Figure 2. (a) Absorption spectra of **1** (black line) and 1e$^-$-oxidized species of **1** (red), 2e$^-$-oxidized species of **1** (purple), 3e$^-$-oxidized species of **1** (blue) in n-C_3H_7CN at 193 K. (b) Spectral change upon reduction of 3e$^-$-oxidized species of **1** (blue) by the addition of 1 equiv of DecFc as the reductant in n-C_3H_7CN at 193 K.

Elemental analysis of **1** confirmed the bulk purity of the crystals and the number of counteranions per cationic moiety.[12] The Ru1···Ru2 distance bridged by the pyrimidine moiety was 6.161(6) Å (Table S1 in the SI), slightly shorter than the Ru···Ru distance in the Creutz−Taube ion (6.88 Å).[13] On the other hand, the Ru1···Ru1′ and Ru2···Ru2′ distances, bridged by one μ-chlorido ligand and two μ-chlorido ligands, are 4.365(5) and 3.626(4) Å, respectively. The latter distance is similar to that of a dinuclear bis(μ-chlorido)ruthenium(II) complex, $[(TPA)Ru^{II}(\mu\text{-}Cl)_2Ru^{II}(TPA)]^{4+}$ [3.648(2) Å].[14]

Cyclic and differential pulse voltammetry (CV and DPV) of **1** were measured in n-C_3H_7CN at 193 K (Figure S4 in the SI). CV of **1** showed four highly reversible and well-separated redox waves with peak separations of 58−74 mV, assigned to the Ru^{II}/Ru^{III} couples of the four Ru centers. The redox potentials ($E_{1/2}$) were determined to be +0.41, +0.78, +0.94, and +1.48 V vs saturated calomel electrode (SCE), and the electric current for each wave corresponded to that of a one-electron (1e$^-$)-redox process based on the DPV peak intensity. To assign the redox processes, density functional theory calculations were performed on **1**, the 1e$^-$-oxidized **1**, and the 2e$^-$-oxidized **1**. Consequently, the first and second oxidations should proceed on the Ru1 and Ru1′ centers with a terminal chlorido ligand at each Ru^{II} center and bridged by one μ-chlorido ligand (Figure S5 in the SI).[12] Therefore, the four redox processes of **1** can be assigned as follows: The lower two waves are due to the redox couples of the Ru1 and Ru1′ centers, and the higher two are ascribed to those of the Ru2 and Ru2′ centers bridged by two μ-chlorido ligands. The assignments are supported by the chemical oxidation experiments to observe IVCT bands (see below).

To confirm the formation of MV states for **1**, we oxidized **1** with tris(4-bromophenyl)ammounium hexachloroantimonate (TBPAH; E_{red} = +1.07 V vs SCE)[15] as a chemical oxidant. The oxidation reactions of **1** with TBPAH performed in n-C_3H_7CN at 193 K were monitored through the absorption spectral changes (Figures 2 and S6 in the SI).[16] In the course of the addition of 0−2 equiv of the oxidant, the UV−vis spectra showed stepwise changes with isosbestic points at 381 nm for 0−1 equiv and 390 nm for 1−2 equiv, whereas IVCT bands were not observed (Figure S6a,b in the SI).[17] In contrast, upon the addition of 2−3 equiv of the oxidant, an IVCT band gradually arose at 1328 nm, and then the isosbestic point was observed at 381 nm.[17] Therefore, electronic coupling between the Ru^{II} and Ru^{III} centers occurred in the MV state of **1** formed by 3e$^-$ oxidation. The IVCT band of the 3e$^-$-oxidized species of **1** disappeared upon reduction with the addition of 1 equiv of decamethylferrocene (DecFc) as a reductant (Figure 2b).

The parameters related to the arguments on MV states are summarized in Table 1. The comproportionation constants (K_c) of the MV states of **1** were estimated using eq 1 to be 1.9×10^6, 520, and 1.4×10^9 for the 1e$^-$-, 2e$^-$-, and 3e$^-$-oxidized species, respectively, based on the difference (ΔE) between the oxidation potential to form the MV state and the subsequent oxidation potential. In addition, the electronic coupling parameter (H_{ab}) for the 3e$^-$-oxidized species of **1** was calculated to be 1868 cm^{-1}, according to the Hush equation in eq 2.[18] The MV parameters

$$K_c = 10^{\Delta E/59\ \mathrm{mV}} \text{ at } 298\ \mathrm{K} \quad (1)$$

$$H_{ab} = 0.0206(\varepsilon_{max}\nu_{max}\Delta\nu_{1/2})^{1/2}/r_{ab} \quad (2)$$

indicate that the MV state formed by 3e$^-$ oxidation of **1** is categorized in the Robin−Day class II,[4] suggesting a partially valence-delocalized situation. The intense IVCT band observed for 3e$^-$-oxidized species of **1** indicates that the electronic interaction between the two Ru centers in the bis(μ-chlorido) dimeric unit in **1** (H_{ab} = 1868 cm^{-1}) should be stronger than those in $[(NH_3)_5Ru^{III}(\mu\text{-pyradine})Ru^{II}(NH_3)_5]^{5+}$ (H_{ab} = 597 cm^{-1}) and $[(NH_3)_5Ru^{III}(\mu\text{-pyrimidine})Ru^{II}(NH_3)_5]^{5+}$ (H_{ab} = 143 cm^{-1}). In contrast, upon 1e$^-$ oxidation of **1**, the formed MV state, where the 3+ charge is localized on one Ru center of the mono(μ-chlorido) dimeric unit, is categorized into class I, despite its large K_c value (Scheme 2).

As for **1**, not only the Ru1···Ru1′ pair bridged by the mono(μ-chlorido) ligand but also the Ru1···Ru2 pair linked by the pyrimidine moiety could show IVCT absorption; in fact, $[(NH_3)_5Ru^{III}(\mu\text{-pyrimidine})Ru^{II}(NH_3)_5]^{5+}$ has been categorized as a class II MV compound (Table 1).[19] The weak electronic interaction between the Ru1 and Ru2 centers bridged by the pyrimidine moiety in **1** is probably derived from distortion of the dinuclear structure including Ru1 and Ru2 in **1**. In the crystal structure of **1**, the Ru1 and Ru2 centers deviate from the pyrimidine mean plane in the syn direction: The deviations from the pyrimidine plane are 0.509 and 0.164 Å for Ru1 and Ru2, respectively (Figure S8 in the SI). This distortion results in a disturbance of the overlapping of the orbitals among the Ru centers and the pyrimidine moiety.

In conclusion, we have synthesized a novel cyclic tetranuclear ruthenium(II) complex, **1**, using bpmpm as the dinucleating ancillary ligand. Complex **1** showed four well-separated reversible redox waves, which were derived from the $Ru^{II/III}$ processes of the four Ru centers. Stepwise oxidations of **1** were performed with a chemical oxidant to observe the three different MV states. The 1e$^-$ and 2e$^-$ oxidations of **1** afforded two kinds of valence-localized complexes in class I MV states; in contrast, the 3e$^-$-oxidized species of **1** was assigned as a class II MV state, where the charge was partially delocalized on the two Ru centers in the bis(μ-chlorido) framework.

dx.doi.org/10.1021/ic502422u | Inorg. Chem. 2014, 53, 12677−12679

Table 1. Metal-to-Metal Distances (r_{ab}), Absorption Maxima (ν_{max}), Half-Height Widths ($\nu_{1/2}$), and Absorption Coefficients (ε_{max}) of IVCT Bands, Electronic Coupling Constants (H_{ab}), Differences between Two Successive Oxidation Potentials (ΔE), and Comproportionation Constants (K_c) for MV Complexes

complex	r_{ab}, Å	ν_{max}, cm^{-1}	$\nu_{1/2}$, cm^{-1}	ε_{max}, M^{-1} cm^{-1}	H_{ab}, cm^{-1}	ΔE, mV	K_c	class
$[(NH_3)_5Ru^{III}(\mu\text{-pym})Ru^{II}(NH_3)_5]^{5+}$ [a]	6.0	7150	6000	41	143	150	340	II
$[(TPA)Ru^{III}(\mu\text{-Cl})_2Ru^{II}(TPA)]^{3+}$ [b]	3.6	9240	4500	120	404	370	1.6×10^6	II
$[(Me_3tacn)Ru^{III}(\mu\text{-Cl})_3Ru^{II}(Me_3tacn)]^{2+}$ [c]	2.9	6250		300		1190	1.0×10^{20}	III
complex **1** (1e$^-$ oxidation)[d]	4.4					370	1.9×10^6	I
complex **1** (2e$^-$ oxidation)[d]	6.2					160	520	I
complex **1** (3e$^-$ oxidation)[d]	3.6	7530	3291	4300	1868	540	1.4×10^9	II

[a]Reference 19, in D_2SO_4/D_2O at room temperature. [b]Reference 20, in CH_3CN at room temperature, electrolyte (0.1 M $TBAPF_6$). [c]Reference 21, in CH_3CN at 293 K, electrolyte (0.1 M $TBAPF_6$). [d]In n-C_3H_7CN at 193 K, electrolyte (0.1 M $TBAPF_6$). pym = pyrimidine, TPA = tris(2-pyridylmethyl)amine, and Me_3tacn = 1,4,7-trimethyl-1,4,7-triazacyclononane.

Scheme 2. Redox Processes Occurring in 1 and Classification of MV States Formed in 1

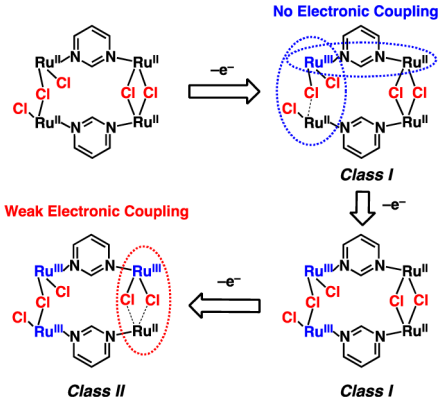

■ ASSOCIATED CONTENT

Ⓢ Supporting Information

Crystallographic data in CIF format, details of the experimental procedure, ESI-TOF-MS, ^1H NMR, and $^1H-^1H$ COSY spectra, CV and DPV, and a side view of **1**, selected bond lengths and angles, and Cartesian coordinates. This material is available free of charge via the Internet at http://pubs.acs.org.

■ AUTHOR INFORMATION

Corresponding Author

*E-mail: kojima@chem.tsukuba.ac.jp.

Notes

The authors declare no competing financial interest.

■ ACKNOWLEDGMENTS

This work was partially supported by Grants-in-Aid 24245011 and 25109507 (to T.K.) and 26-2424 (to S.O.) from the Japan Society of Promotion of Science (JSPS, MEXT) of Japan. T.K. also appreciates financial support from The Mitsubishi Foundation.

■ REFERENCES

(1) (a) Dubois, M. R. *Chem. Rev.* **1989**, *89*, 1−9. (b) Martell, A. E.; Perutka, J.; Kong, D. *Coord. Chem. Rev.* **2001**, *216*, 55−63.

(2) (a) Thompson, L. K. *Coord. Chem. Rev.* **2002**, *233*, 193−206. (b) Popescu, D.-L.; Chanda, A.; Stadler, M.; Oliveira, F. T. D.; Ryabov, A. D.; Munck, E.; Bominaar, E. L.; Collins, T. J. *Coord. Chem. Rev.* **2008**, *252*, 2050−2071.

(3) (a) Demadis, K. D.; Hartshom, C. M.; Meyer, T. J. *Chem. Rev.* **2001**, *101*, 2655−2685. (b) Brunschwig, B. S.; Creutz, C.; Sutin, N. *Chem. Soc. Rev.* **2002**, *31*, 168−184. (c) D'Alessandro, D. M.; Keene, F. R. *Chem. Rev.* **2006**, *106*, 2270−2298.

(4) Robin, M. B.; Day, P. *Adv. Inorg. Chem. Radiochem.* **1967**, *10*, 247−422.

(5) (a) Sessoli, R.; Gatteschi, D.; Caneschi, A.; Novak, M. A. *Nature* **1993**, *365*, 141−143. (b) Cukiernik, F. D.; Luneau, D.; Marchon, J.-C.; Maldivi, P. *Inorg. Chem.* **1998**, *37*, 3698−3704.

(6) (a) Nemykin, V. N.; Rohde, G. T.; Barrett, C. D.; Hadt, R. G.; Bizzarri, C.; Galloni, P.; Floris, B.; Nowik, I.; Herber, R. H.; Marrani, A. G.; Zanoni, R.; Loim, N. M. *J. Am. Chem. Soc.* **2009**, *131*, 14969−14978. (b) Jaio, J.; Long, G. J.; Grandjean, F.; Beatty, A. M.; Fehlner, T. P. *J. Am. Chem. Soc.* **2003**, *125*, 7522−7523.

(7) (a) Serroni, S.; Campagna, S.; Denti, G.; Keyes, T. E.; Vos, J. G. *Inorg. Chem.* **1996**, *35*, 4513−4518. (b) Afrati, T.; Dendrinou-Samara, C.; Raptopoulou, C. P.; Terzis, A.; Tangoulis, V.; Kessissoglou, D. P. *Angew. Chem., Int. Ed.* **2002**, *41*, 2148−2150. (c) Klingele, J.; Dechert, S.; Meyer, F. *Coord. Chem. Rev.* **2009**, *253*, 2698−2741. (d) Schneider, B.; Demeshko, S.; Neudeck, S.; Dechert, S.; Meyer, F. *Inorg. Chem.* **2013**, *52*, 13230−13237.

(8) Lau, V. C.; Berben, L. A.; Long, J. R. *J. Am. Chem. Soc.* **2002**, *124*, 9042−9043.

(9) (a) Nihei, M.; Ui, M.; Oshio, H. *Polyhedron* **2009**, *28*, 1718−1721. (b) Oshio, H.; Onodera, H.; Ito, T. *Chem.—Eur. J.* **2003**, *9*, 3946−3950.

(10) Gruenwedel, D. W. *Inorg. Chem.* **1968**, *7*, 495−501.

(11) Oshio, H.; Ichida, H. *J. Phys. Chem.* **1995**, *99*, 3294−3302.

(12) See the SI.

(13) Creutz, C.; Taube, H. *J. Am. Chem. Soc.* **1969**, *91*, 3988−3989.

(14) Kojima, T.; Amano, T.; Ishii, Y.; Ohba, M.; Okaue, Y.; Matsuda, Y. *Inorg. Chem.* **1998**, *37*, 4076−4085.

(15) Tfouni, E. *Coord. Chem. Rev.* **2000**, *196*, 281−305.

(16) Trials to detect electron spin resonance signals assignable to those of the MV species at 4 K were not successful.

(17) Different isosbestic points observed for each oxidation step of **1** suggest that disproportionation equilibria do not exist among the oxidation states. Additionally, electrolysis of **1** at appropriate potentials afforded the same UV−vis spectra as those of the corresponding species formed by chemical oxidation (Figure S7 in the SI).

(18) (a) Hush, N. S. *Prog. Inorg. Chem.* **1967**, *8*, 391−444. (b) Hush, N. S.; Parashad, R.; Yadav, S. K. S.; Agarwala, U. *J. Inorg. Nucl. Chem.* **1981**, *43*, 2359−2374.

(19) Richardson, D. E.; Taube, H. *J. Am. Chem. Soc.* **1983**, *105*, 40−51.

(20) Makino, M.; Ishizuka, T.; Ohzu, S.; Hua, J.; Kotani, H.; Kojima, T. *Inorg. Chem.* **2013**, *52*, 5507−5514.

(21) Neubold, P.; Vedova, B. S. P. C. D.; Wieghardt, K.; Nuber, B.; Weiss, J. *Inorg. Chem.* **1990**, *29*, 3355−3363.